NASA Technical Memorandum 58276

Euler Solutions Using an Implicit Multigrid Technique

Chien-peng Li

November 1986

(NASA-TM-58276) EULER SOLUTICNS USING AN IMPLICIT MULTIGRID TECHNIQUE (NASA) 19 p CSCL 01A

N87-16792

Unclas
G3/02 43750

NASA
National Aeronautics and
Space Administration

Lyndon B. Johnson Space Center
Houston, Texas

NASA Technical Memorandum 58276

Euler Solutions Using an Implicit Multigrid Technique

Chien-peng Li
Lyndon B. Johnson Space Center
Houston, Texas

NASA
National Aeronautics and
Space Administration

Scientific and Technical
Information Branch

1986

CONTENTS

FIGURES

ABSTRACT

A coarse-grid correction algorithm has been implemented into an implicit upwind Euler solver and tested for transonic airfoil problems. The Euler solver uses split-flux formulation and pentadiagonal scalar equations, respectively, for the explicit and implicit operators. The multigrid sequence starts at the fine grid level, then steps down to each coarse grid level to smooth error components using implicit operators. An estimate of residuals can be obtained by two approaches, which differ in the level at which the residuals are collected. Both approaches will lead to a work reduction factor of 12 for a Mach 0.75 flow at 2° incidence angle on a 65 × 26 grid. The work reduction factor is found to increase in proportion to the number of grid levels.

INTRODUCTION

The multigrid (MG) method was first advocated in 1980 by Brandt (ref. 1) as a potentially efficient technique to solve fluid dynamics equations. Since then, Ni has developed an innovative explicit scheme to solve the Euler equations, and Jameson and his coworkers (ref. 3) have attempted to combine the MG strategy with explicit as well as with implicit schemes. Jameson's latest work has shown an impressive work reduction factor (WRF) as great as 15 for a nonlifting transonic airfoil flow on a 128 × 32 grid. These applications share two prominent features; namely, the finite-volume formulation and the centered difference approximation to the conventional flux terms. Thereby, the error components can be removed and expelled out the computation domain very effectively on a succession of grid levels and smoothed by the numerical damping added to the difference operators. It is of interest to determine whether the MG strategy will work equally well if the flux terms are split into subflux terms according to their eigenvalues and approximated by upwind schemes. Because the directional preference of signal propagation might be lost by collecting residuals on coarse grids and the numerical damping is generally not required to stabilize the results near the shock, the basic mechanisms attributable to the removal of error components seem to be missing. To resolve the unsettling issues, the author has incorporated the multigrid sequencing into an ADI factorization Euler solver and reported the findings in a 1984 paper (ref 4). The MG algorithm is different from other versions in using the corrections at each level rather than the residuals at the fine grid level. Although the algorithm is stable, as well as easy to implement, and requires no additional storage for intermediate variables, the improvement in WRF is relatively small compared to others. It has been found in this study that a much higher WRF can be obtained by introducing local time increment and implicit damping to the algorithm.

SPLIT-FLUX EULER FORMULATION

The conservation-law form of the inviscid flow equations is given in generalized coordinates ξ and η.

$$u_t + F_\xi + G_\eta = 0 \tag{1}$$

Each part of the flux term is composed of three subflux terms which are associated with local characteristics $\lambda_\xi, \lambda_\eta$. They are of the following form.

$$\bar{F} = J\rho \sum_{\ell=-1}^{1} \left(\gamma \lambda_\xi\right)_\ell \begin{bmatrix} 1 \\ u + \ell c \bar{\xi}_x \\ v + \ell c \bar{\xi}_y \\ q + \ell \bar{u} c/\bar{\xi} + |\ell| \gamma e \end{bmatrix}, G = J\rho \sum_{\ell=-1}^{1} \left(\gamma \lambda_\eta\right)_\ell \begin{bmatrix} 1 \\ u + \ell c \bar{\eta}_x \\ v + \ell c \bar{\eta}_y \\ q + \ell \bar{v} c/\bar{\eta} + |\ell| \gamma e \end{bmatrix} \quad (2)$$

where $\gamma_\ell = (1 - |\ell|)(\gamma - 1)/\gamma + |\ell|/(2\gamma)$, $\lambda_{\xi\ell} = \bar{u} + \ell c \bar{\xi}$, $\lambda_{\eta\ell} = \bar{v} + \ell c \bar{\eta}$,

$$\bar{u} = \xi_x u + \xi_y v,\ \bar{v} = \eta_x u + \eta_y v,\ \bar{\xi}_x = \xi_x/\bar{\xi},\ \bar{\xi} = \left(\xi_x^2 + \xi_y^2\right)^{1/2}, \text{etc.}$$

and $\bar{\xi}_x, \bar{\xi}_y, \bar{\eta}_x, \bar{\eta}_y$ are treated as local invariants. The three parts corresponding to the characteristic values can be cast alternately in the following form.

$$\bar{F} = J \frac{\gamma - 1}{\gamma} \bar{u} \begin{bmatrix} \rho \\ \rho u \\ \rho v \\ \rho q \end{bmatrix} + J \frac{\bar{u} \pm c\bar{\xi}}{2\gamma} \begin{bmatrix} \rho \\ \rho(u \pm c\bar{\xi}_x) \\ \rho(v \pm c\bar{\xi}_y) \\ \rho q + \dfrac{\gamma}{\gamma - 1} p + \rho \bar{u} c/\bar{\xi} \end{bmatrix}$$

$$\bar{G} = J \frac{\gamma - 1}{\gamma} \bar{v} \begin{bmatrix} \rho \\ \rho u \\ \rho v \\ \rho q \end{bmatrix} + J \frac{\bar{v} \pm c\bar{\eta}}{2\gamma} \begin{bmatrix} \rho \\ \rho(u \pm c\bar{\eta}_x) \\ \rho(v \pm c\bar{\eta}_y) \\ \rho q + \dfrac{\gamma}{\gamma - 1} p \pm \rho \bar{v} c/\bar{\eta} \end{bmatrix}$$

Standard notation is used for flow variables; viz, the density ρ, the pressure p, and the velocity components u and v in Cartesian coordinates, the total internal energy ε and $(q = u^2 + v^2)/2$, and the internal energy $e = C_v T$, which relates to p and ρ by the equation of state. The sonic speed is $c = (\gamma p/\rho)^{1/2}$; γ is the ratio of specific heats. The integer ℓ is used to simplify the equation form, in which each characteristics component can be identified by ℓ = -1, 0, 1. The conventional matrix of characteristics has four components:

$$\Lambda_\xi = \text{diag}\,(\bar{u} - c\bar{\xi}, \bar{u}, \bar{u}, \bar{u} + c\bar{\xi}),\ \ \Lambda_\eta = \text{diag}\,(\bar{v} - c\bar{\eta}, \bar{v}, \bar{v}, \bar{v} + c\bar{\eta})$$

In accordance with the sign of the characteristics, second-order one-sided difference equations are used upstream or downstream at each grid point. The order of accuracy is the same on the boundary points as those in the field. Details of boundary treatment are given in reference 4 and a forthcoming publication.

UPWIND FACTORIZATION TECHNIQUE

Let Δv and Δu denote the unknown correction vectors abbreviated for $(\Delta\rho, \Delta u, \Delta v, \Delta e)^T$ and $(\Delta\rho, \Delta\rho u, \Delta\rho v, \Delta\rho\varepsilon)^T$, respectively. The solution procedure for implicit calculation can be described in the following four steps:

$$
\begin{aligned}
&\Delta v_{i,j} = \left(P^{-1} r\right)_{i,j} \\
&\left(I + \Delta t \delta_\xi \Lambda_\xi - d_i \delta_{\xi\xi}\right) \Delta w_{i,j} = \left(T^{-1} \Delta v\right)_{i,j} \\
&\left(I + \Delta t \delta_\eta \Lambda_\eta - d_i \delta_{\eta\eta}\right) \Delta w^*_{i,j} = \left(S^{-1} T \Delta w\right)_{i,j} \\
&\Delta v_{i,j} = (S \, \Delta w^*)_{i,j}
\end{aligned}
\tag{3}
$$

where r refers to the residual vector obtained from the explicit operation in equations (1) and (2) after replacing the derivatives of flux terms by their difference formulas. The subscripts i and j denote the spatial location of a grid point network ranging from $i = 1$ to $imax$ and $j = 2$ to $jmax$. The operators δ_ξ and δ_η are for upwind difference and $\delta_{\xi\xi}$, $\delta_{\eta\eta}$ are for centered difference associated with a damping coefficient, d_i. The difference formulas stop switching sides if the magnitude of the characteristics is smaller than a prescribed tolerance in order to reduce the truncation errors near the stagnation and sonic points. The notation used and the expanded form of the second and third equations in equation (3) are given in reference 5. The step increment is generally $\Delta t = CFL \cdot min$ $(\Delta\xi/|\Lambda_\xi|_\ell, \Delta\eta/|\Delta_\eta|_\ell)$ where CFL is the Courant number. It must be equal to or less than 0.25 if implicit operations are skipped. A global Δt implies that one value of time increment is used for the entire domain; a local Δt is obtained at each point and used at that point.

MULTIGRID ALGORITHM

The implicit procedure for single-level grid calculations may be summarized as follows:

$$
\begin{aligned}
L \, \Delta v^{k+1}_{i,j} &= r^k_{i,j} \\
v^{k+1}_{i,j} &= v^k_{i,j} + \Delta v^{k+1}_{i,j}
\end{aligned}
\tag{4}
$$

where L is the operator representing equation (3) and $r_{i,j}$, $\Delta v_{i,j}$ are called the residual and correction vectors, respectively. On a coarse grid with spacing twice as large as in all coordinates, equation (4) becomes

$$
\begin{aligned}
L \, \Delta v_{2h} &= W^{2h}_h \, r_h \qquad \text{or} \\
&= W^{2h}_h \, \Delta v_h
\end{aligned}
\tag{5}
$$

On a still coarser grid,

$$L\,\Delta v_{4h} = W_{2h}^{4h}\left[\left(W_h^{2h} r_h - T_h^{2h} r_h\right) + \Delta v_{2h}\right]$$

$$L\,\Delta v_{8h} = W_{4h}^{8h}\left[W_{2h}^{4h}\left(W_h^{2h} r_h - T_h^{2h} r_h\right) + \Delta v_{4h}\right]$$

etc., where W is an operator representing the weighted average of the residuals and corrections on the grid points surrounding the coarser grid point, and T is an operator transferring directly the values from fine to coarse grid. The correction obtained at each level is interpolated back to the fine grid by

$$v_h = v_h + I_{2h}^{h}\,\Delta v_{2h} \tag{6}$$

The implicit operator I is a linear function on the boundaries and bilinear inside the domain. The weighted operator W serves a very important role to eliminate high frequency modes before passing the residuals to coarser grids. Equation (5) is in a general form so that the residuals may be obtained from either r or Δv, or from both. For example, letting

$$W_h^{2h} = T_h^{2h} \quad \text{and} \quad W_{2h}^{4h} = T_{2h}^{4h} \quad \text{etc.}$$

The present MG strategy uses the explicit residuals only once on the fine grid level, then uses the implicit corrections on other grid levels. A complete cycle of the MG algorithm is illustrated in figure 1.

DISCUSSION

To help evaluate the performance of the implicit MG algorithm, three parameters $(\Delta\rho/\rho)max$, number of supersonic points NSUP, and stagnation pressure P_t are used for monitoring the convergence rate, whereas P_t and Mach contours are used for checking solution accuracy. Several grids (113×34, 97×34, 65×26, 65×22) have beeen considered, but most of the results shown here are based on a 65×26 grid and for the NACA 0012 airfoil. The baseline calculation uses global Δt with $CFL = 10$, as it encounters stability difficulties with local Δt even with $CFL = 2$. Figure 2 shows the convergence history and results of a non-lifting case. The magnitude of $(\Delta\rho/\rho)$ in the MG calculation is typified by a plateau two orders higher than that in the single-grid (SG) calculation. Nevertheless, the MG calculation is at least four times as efficient as the single-grid calculation. The WRF is close to 7 if optimal values of $CFL = 4$ and $d_i = 1$ are used instead. Figure 3 shows the 65×26 grid and the Mach contours for a Mach 0.8 flow at 1.25° incidence angle. Figure 4 is a comparison of the convergence rate between the calculations made from the MG algorithm with $CFL = 2$ local Δt and from the single-grid algorithm with $CFL = 10$. The WRF is estimated to be 7 for this case and could have been 13 if $CFL = 4$ had been used. Note the sharpness of the shock above the airfoil and the compression wave underneath. The accuracy of the current results seems to be on a par with the conventional SG solution on a 128×32 grid.

If the MG algorithm uses the explicit residuals on coarse grids; viz,

$$L \, \Delta v_{2h} = W_h^{2h} \, r_h$$

the convergence rate is nearly equivalent to that of the current algorithm. Shown in figure 5 is the comparison between the two. A comparison of different types of residual collection is shown in figure 6. It is seen that the use of local time step increment substantially accelerates the convergence rate.

In the following table the converged values of pressures on the surface and of NSUP are listed. The slight differences seen are partly caused by the peculiar behavior of the solution technique (eq. (3)), whereby the factorization error affects the converged solutions.

Parameter	P_t	1 Level	2 Levels	3 Levels
Work unit Wu		1000	200	116
P_{max}	39.46	40.11	38.96	38.72
P_{min}		15.01	14.59	14.78
NSUP		86	88	88

$M = 0.75, \alpha = 2°$; 65×26, 33×14, 17×8 grids

CONCLUSIONS

The current MG algorithm is capable of enhancing the stability and the efficiency of the ADI factorization technique, and of retaining the excellent shock-capturing capability rendered by the split-flux formulation. Satisfactory results are obtained from a 65×26 grid for Mach 0.75 flow at 2° incidence angle with a work reduction factor equal to 12. The apparent shortcoming of the algorithm is in the difficulty of lowering the maximum incremental vector further after a reasonable number of iterations.

REFERENCES

1. Brandt, A.: Multi-Level Adaptive Computations in Fluid Dynamics. AIAA J., vol. 18, no. 10, Oct. 1980, pp. 1165-1172.

2. Ni, R. H.: A Multiple Grid Scheme for Solving the Euler Equations. AIAA J., vol. 20, no. 11, Nov. 1982, pp. 1565-1571.

3. Jameson, A.; and Yoon, S.: Multigrid Solution of the Euler Equations Using Implicit Schemes. AIAA Paper 85-0293, AIAA 23rd Aerospace Sciences Meeting, Jan. 14-17, 1985.

4. Li, C. P.: A Multigrid Factorization Technique for the Flux-Split Euler Equations. Proceedings of the Ninth Inter. Conf. on Numerical Methods for Fluid Dynamics, Lectures in Physics, vol. 218, Springer-Verlag, Jan. 1985, pp. 375-379.

5. Li, C. P.: A Finite-Difference Method for Solving Transient Viscous Flow Problems. AIAA J., vol. 23, no. 5, 1985, pp. 659-668 .

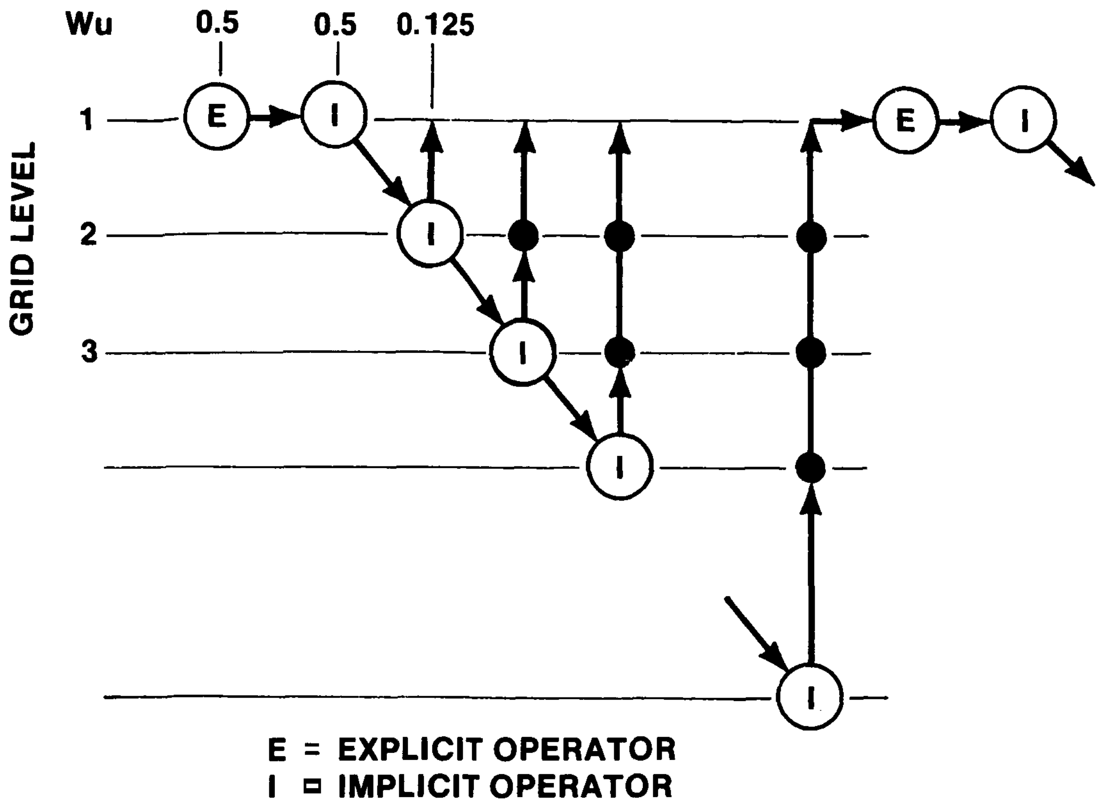

Figure 1.- Schematic of a complete MG cycle.

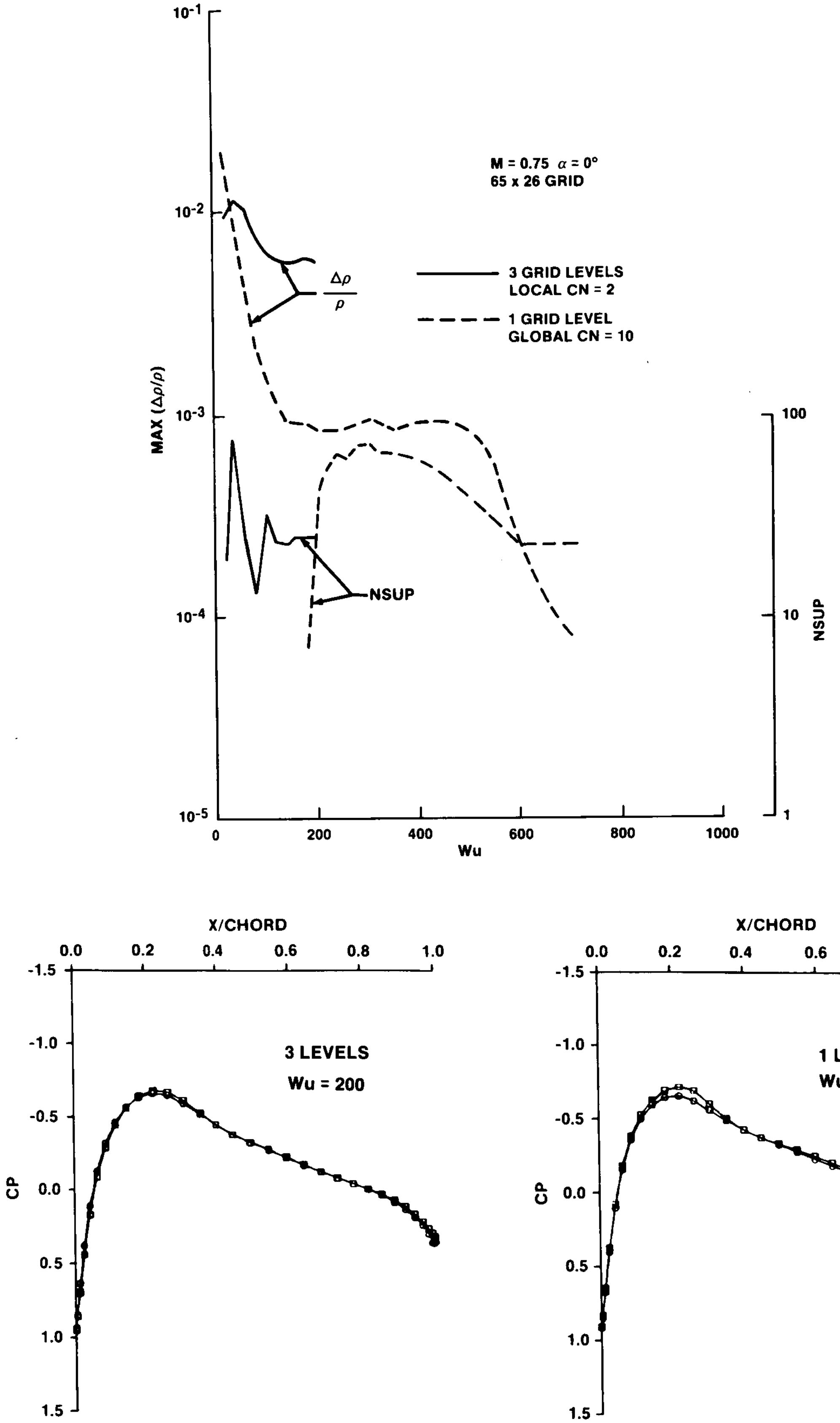

Figure 2.- Comparisons of single-grid and multigrid results.

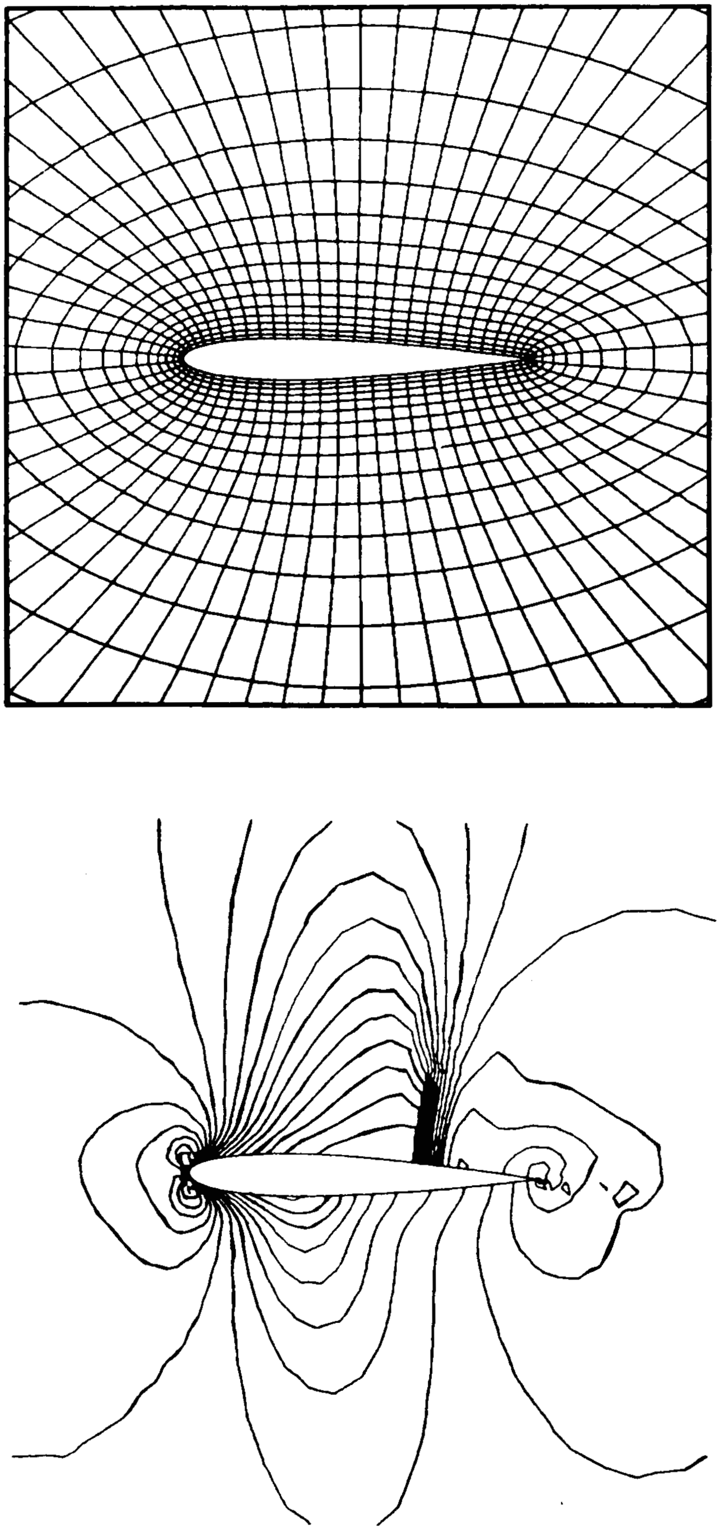

Figure 3.- Grid and Mach contours for $M = 0.8, \alpha = 1.25°$ calculation.

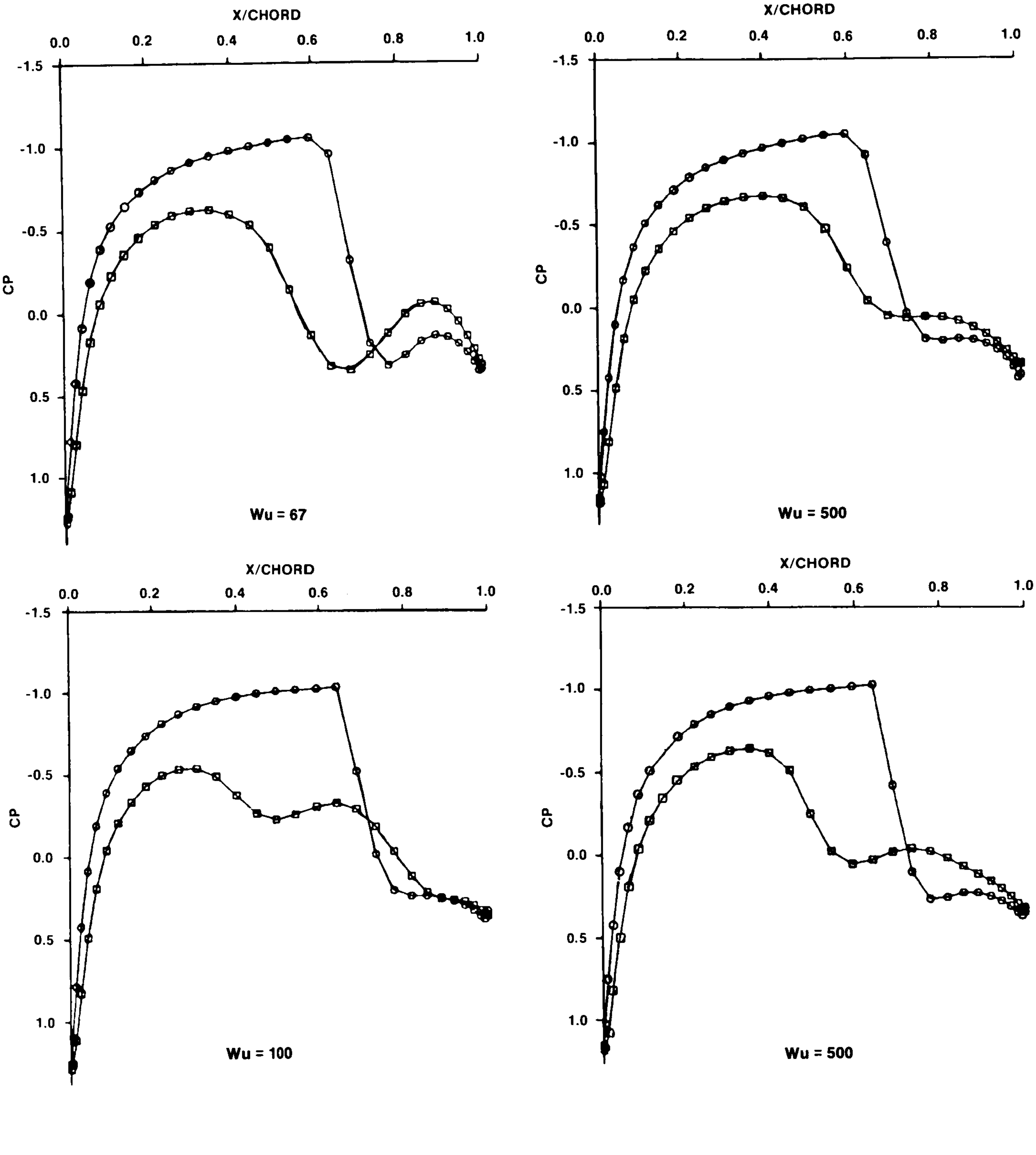

Figure 4.- Comparison of convergence history between single-grid and multigrid calculations.

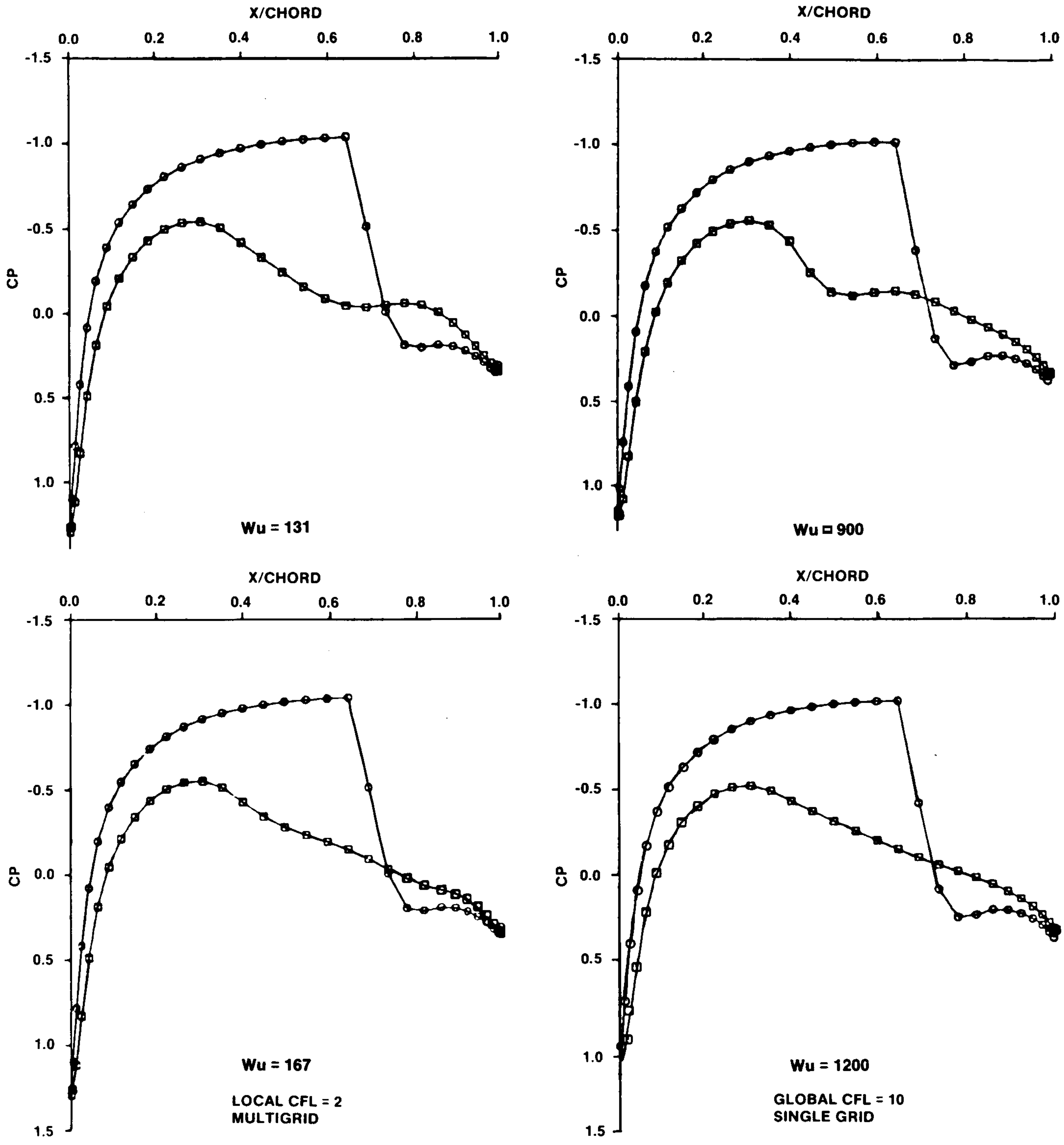

Figure 4.- Concluded

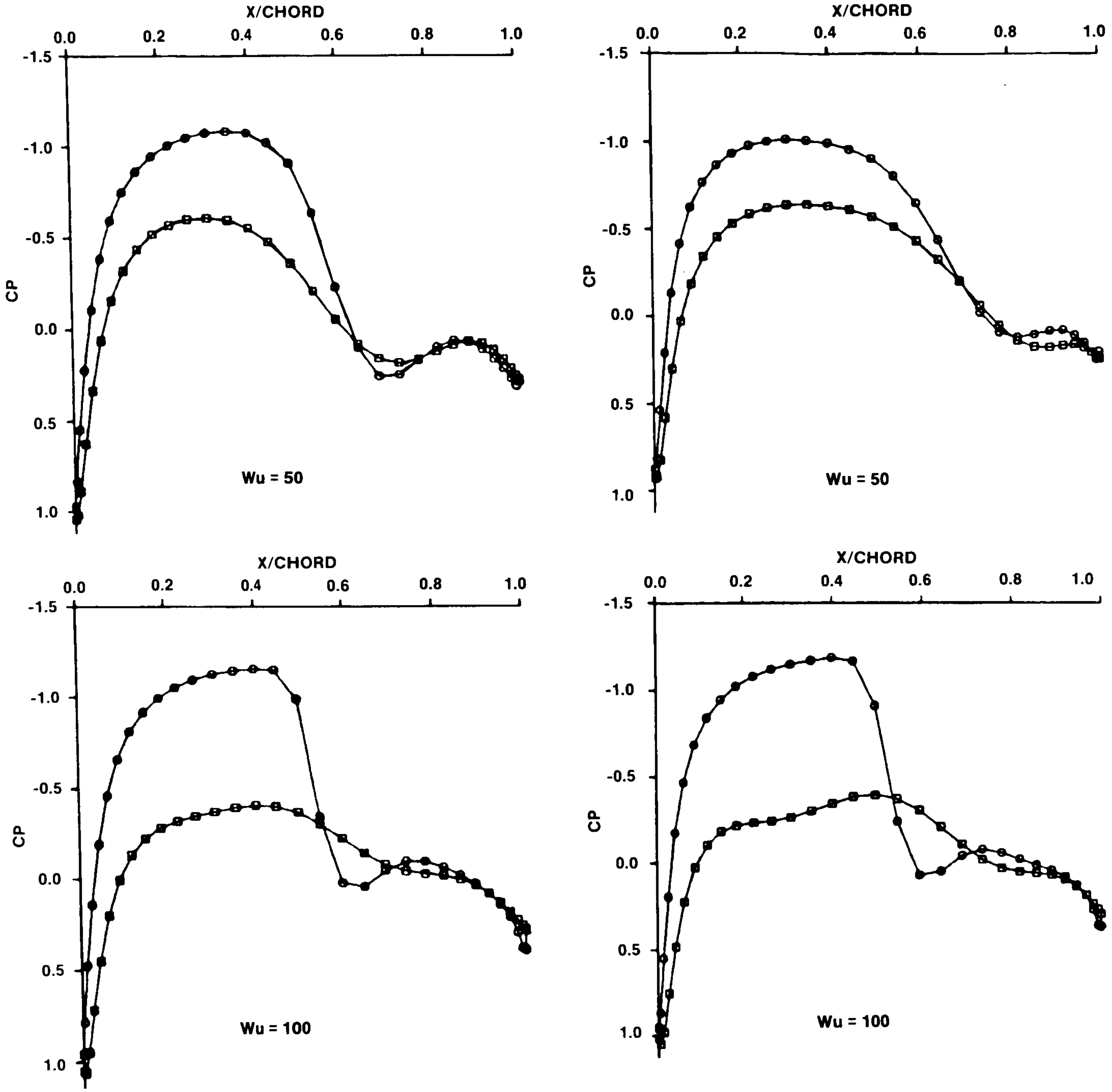

Figure 5.- Comparison of convergence rate between two estimates of residuals.

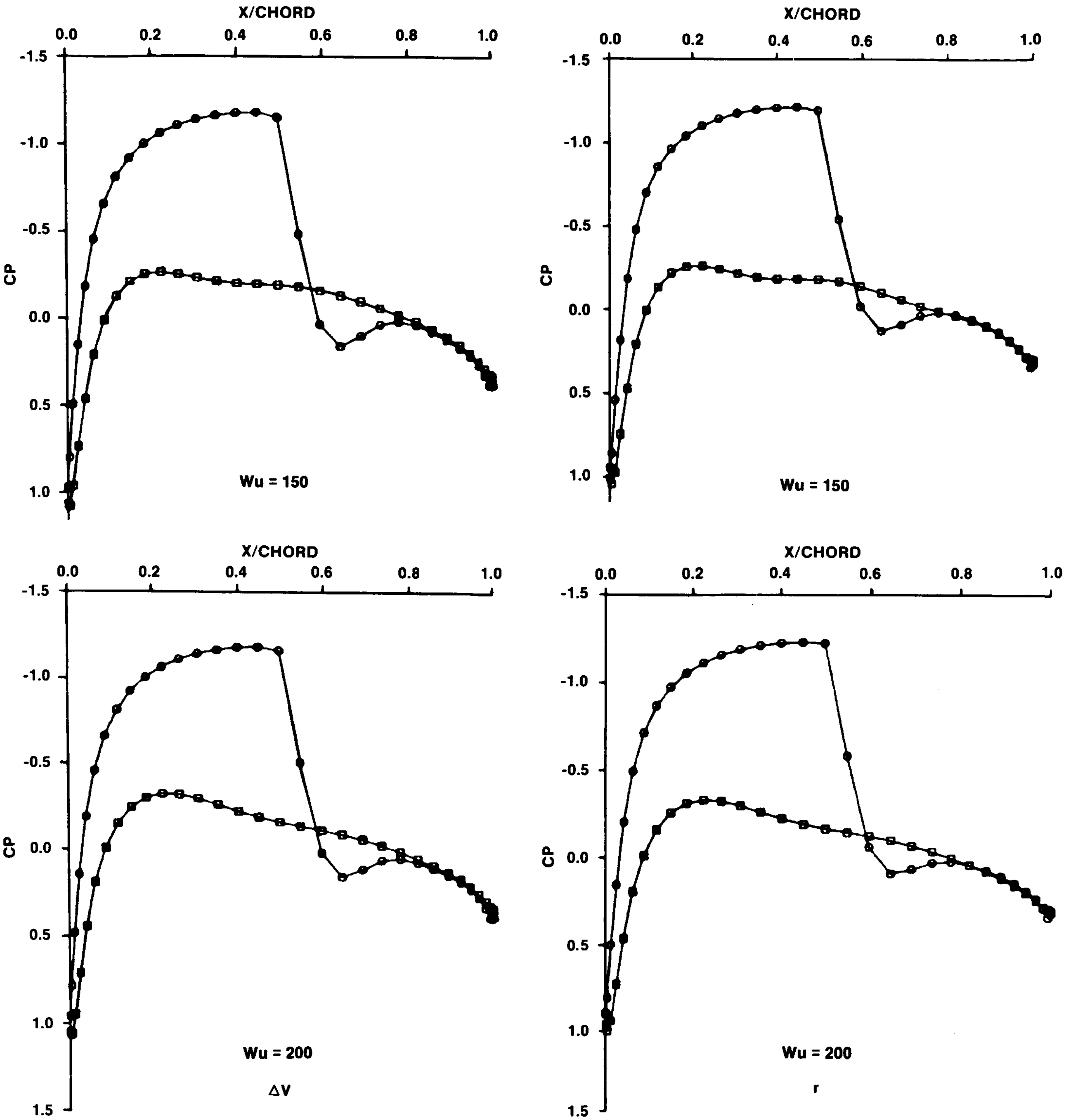

Figure 5.- Concluded

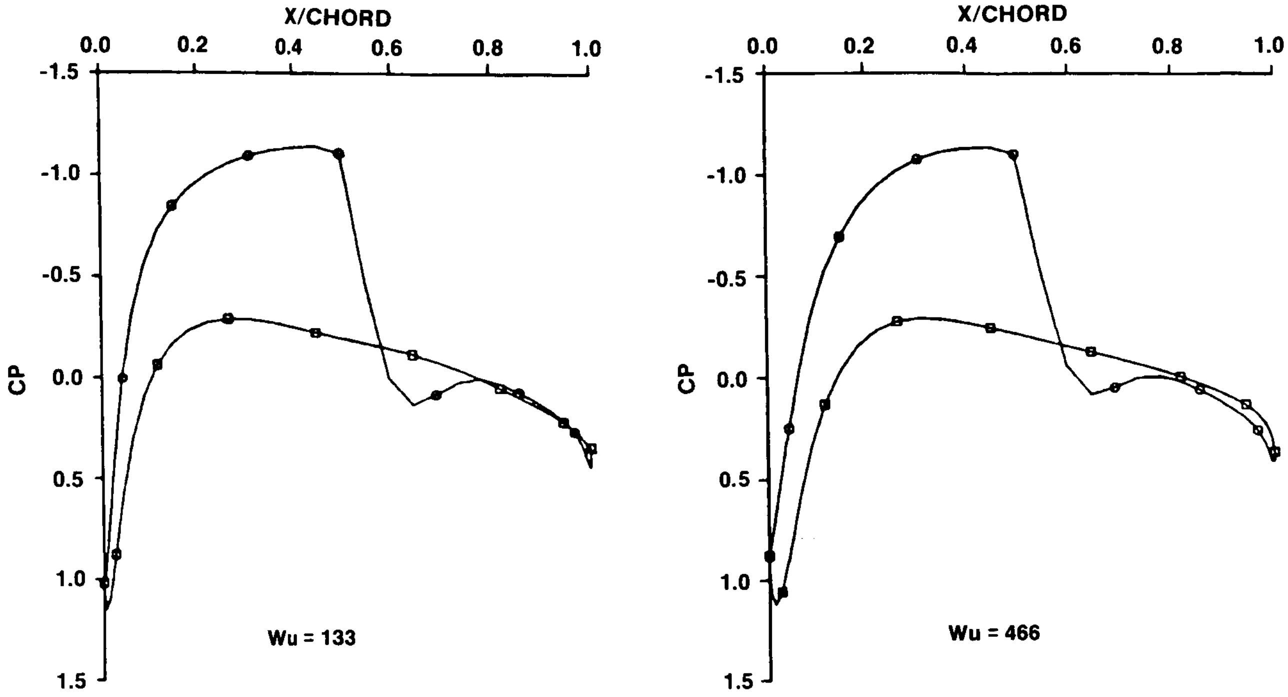

(a) $r_{2h} = W_h^{2h}\,\Delta v_h$; $CFL = 4$, local.

(b) $r_{2h} = T_h^{2h}\,\Delta v_h$; $CFL = 10$, global.

Figure 6.- Comparisons of MG results using different types of residual collections.

1. Report No.	2. Government Accession No.	3. Recipient's Catalog No.
NASA TM-58276		

4. Title and Subtitle	5. Report Date
EULER SOLUTIONS USING AN IMPLICIT MULTIGRID TECHNIQUE	November 1986
	6. Performing Organization Code S-556
7. Author(s) Chien-peng Li	8. Performing Organization Report No.
9. Performing Organization Name and Address Lyndon B. Johnson Space Center Houston, Texas 77058	10. Work Unit No.
	11. Contract or Grant No.
12. Sponsoring Agency Name and Address National Aeronautics and Space Administration Washington, D.C. 20546	13. Type of Report and Period Covered Technical Memorandum
	14. Sponsoring Agency Code

15. Supplementary Notes

Presented at the Second Copper Mountain Multigrid Conference
March 31-April 3, 1985

16. Abstract

A coarse-grid correction algorithm has been implemented into an implicit upwind Euler solver and tested for transonic airfoil problems. The Euler solver uses split-flux formulation and penta-diagonal scalar equations, respectively, for the explicit and implicit operators. The multigrid sequence starts at the fine grid level, then steps down to each coarse grid level to smooth error components using implicit operators. Estimate of residuals can be obtained by two approaches, which differ in the level where the residuals are collected. Both approaches will lead to a work reduction factor of 12 for a Mach 0.75 flow at 2 degrees incidence on a 65x26 grid. The work reduction factor is found to increase proportional to the number of grid levels.

17. Key Words (Suggested by Author(s))	18. Distribution Statement
Finite-difference Multigrid Implicit method Transonic airfoil flow	Unclassified - Unlimited Subject Category 02

19. Security Classif. (of this report)	20. Security Classif. (of this page)	21. No. of Pages	22. Price*
Unclassified	Unclassified	18	

*For sale by the National Technical Information Service, Springfield, Virginia 22161